JOURNAL OF MATERIALS SCIENCE 35 (2000) 5581 – 5585

Mechanical properties of undercooled $Cu_{70}Ni_{30}$ alloy

JINFU LI, YAOHE ZHOU
School of Materials Science and Engineering, Shanghai Jiao Tong University, Shanghai 200030, People's Republic of China
E-mail: jfli@mail1.sjtu.edu.cn

GENCANG YANG
State Key Laboratory of Solidification Processing, Northwestern Polytechnical University, Xi'an, Shaanxi 710072, People's Republic of China

A series of $Cu_{70}Ni_{30}$ alloy ingots, each weighing 650 g, were solidified with various undercoolings prior to nucleation. The material was mechanically tested in the as-solidified condition. Although the decrease of dendrite segregation with increasing undercooling is favorable for the improvement of mechanical properties, the sophisticated evolution of structural morphology leads to a non-monotonic change of both elongation and strength. The maximum tensile strength is obtained in the quasi-spherical structure which forms above the critical undercooling 200 K, while the maximum elongation occurs in the longitudinal tension of the columnar dendrite structure solidified at undercooling 180 K.

1. Introduction

Rapid solidification can give the materials quite distinct structures and properties from those obtained at slow solidification rate, and hence has aroused the interest of researchers. Two kinds of methods have been adopted to get the rapid solidification rate: rapidly quenching or undercooling the melt. To date, although the method of rapid quenching of melt has been applied in an industrial scale, it is exactly confined to the preparation of very thin ribbons, filaments and powders due to the limit of heat extraction [1]. In contrast, the solidification rate is no longer controlled only by the external heat extraction if an alloy melt is substantially undercooled prior to nucleation, which makes high undercooling become an effective technique to produce bulk rapidly solidified alloys [2]. Now some alloys weighing several kilograms have been undercooled to several hundred degrees [3, 4]. A single crystal superalloy turbine blade of excellent quality has been produced with a so-called autonomous directional solidification of the undercooled melt in a special shell mold whose inside surface is covered with an amorphous nucleation inhibiting layer [5].

Another advantage of high undercooling is to make it possible for researchers to in-situ diagnose the rapid solidification process, which has provided us substantial quantitative knowledge of crystal nucleation, growth and morphologies as the functions of undercooling [6, 7]. Howevr, only a few investigations dealt with the properties of the undercooled alloys. This tendency was enhanced after the eighties, from then containerless solidification through electromagnetic levitation melting and drop tube being widely used with the aim of the ground simulation for space processing of materials. In the case of containerless solidification, the size of samples is generally small, and is not favorable for the measurement of some properties. The general view on the mechanical properties of undercooled single phase alloys is that, with undercooling increasing, they will increase correspondingly as the consequence of the decreases of the solute segregation as well as the secondary arm spacing [8]. In fact, the recent studies have demonstrated that the solidification structure of undercooled single phase alloys changes with undercooling sophisticatedly [9, 10]. So the structure dependent mechanical properties need to be investigated systematically.

2. Experimental

The single phase alloy chosen for experiment was $Cu_{70}Ni_{30}$. The preparation and undercooling of the alloy were conducted in a high frequency induction unit. In an experiment run the sodium borosilicate glass used as denucleating agent was first melted with the help of a graphite heater in a fused silica crucible of 40 mm in inside diameter and 100 mm in height. Part of Cu and Ni charges purer than 99.99% were then added in the crucible and *in-situ* melted under the protection of the glass. Subsequently the crucible was transferred in a refractory material sheath on whose side a round hole of 6 mm in diameter had been opened. Through this hole temperature was supervised by an infrared pyrometer. After the temperature was rose higher than the liquidus temperature of the alloy again, the rest of the charges weighing 650 g in total were added. The desired undercooling was achieved in the following superheating-cooling cycles. Temperature distribution in the sample was also investigated by setting three thermocouples at three different points: the center, the midpoint of the radius and the surface at the half of the height of samples. The measurement result indicated that the temperature difference in the radial direction, especially before solidification, was not large. However, we still inserted a thermocouple at the midpoint of the radius in the experiment, and chose the temperature and the structure at this point for study.

The specimen used for measuring mechanical properties was cut from the as-solidified ingot along the longitudinal direction, as near the surface of the ingot as possible, so were free of the manifest microporosity. The specimen of 10 mm in diameter was then machined into the standard tensile bar with a gage length of 30 mm and diameter of 6 mm. In the present work, the 0.2 percent offset yield strength $\sigma_{0.2}$, the ultimate tensile strength σ_b, and the elongation δ were measured by Instron testing machine. Any normal property was represented by the average value of three measurements.

Sometimes the structure of the ingot consisted of columnar crystals, and the nucleation point was generally at the top corner of the ingot since the temperature at this location was the lowest during cooling. In this case the measurement result was influenced by the cutting position of the specimen. When the cutting position near the nucleation point, the columnar crystals were approximately parallel to the tensile direction. We marked this specimen and its properties with "longitudinal", while the specimen far away from the nucleation position and its properties were marked with "transverse" (Fig. 1). For the ingot whose structure was comprised of the equiaxed crystals, we cut the specimens randomly along the outer peripheral direction of the ingot.

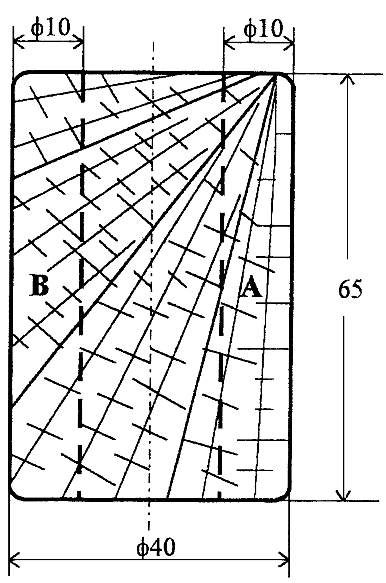

Figure 1 Cutting position of specimens in the as-solidified ingots A—longitudinal; B—transverse.

3. Results and discussions

3.1. Structural transition with undercooling

As described in the previous work [9], the solidification structure of $Cu_{70}Ni_{30}$ alloy changes with the undercooling prior to nucleation. Fig. 2 shows the typical microstructures. When solidification is performed in an ordinary way, there is not obvious undercooling observed in the cooling curve. The structure consists of equiaxed dendritic crystals with coarse branching arms. Slightly increasing undercooling give rise to the increase of grain size but the decrease of secondary dendrite arm spacing (Fig. 2a). However, as undercooling becomes higher than 26 K, some of dendrite arms are disintegrated due to remelting [9, 11]. The structure is refined completely in the undercooling range of 36–80 K (Fig. 2b). If undercooling increases continuously, the grain size rises again. In the undercooling range of 120–175 K, as shown in Fig. 1, formed is very coarse columnar grains containing well-developed dendritic substructures (Fig. 2c). Another decrease of grain size begins at undercooling 175 K, however, the columnar morphology can maintain to the undercooling 180 K. Above the critical undercooling 200 K, the structure consists of the fine quasi-spherical grains in which dendritic substructure exists (Fig. 2d).

3.2. Solute segregation

Solute segregation in solid originates from the nonequilibrium crystallization. Its extent can be described by the segregation ratio which equals the ratio of the solute content at the center of the dendrite arm to that at the interdendritic space when the as-solidified structure consists of dendrites, or the ratio of the solute content at the center of grain to that at gain boundary when structure is free of dendrites. The segregation ratio of undercooled $Cu_{70}Ni_{30}$ is shown in Fig. 3.

As a melt is cooled below the equilibrium melting temperature, driving force for crystallization is accumulated. As a consequence the undercooled melt will first undergo a rapid solidification stage in which the concentrated release of the latent heat leads to the temperature recalescence of the system. The recalescence makes the dendritic skeleton in the superheated state immediately as soon as they form. The solute content has to change toward the equilibrium solidus concentration, otherwise the solid will be remelted. In fact, the partial remelting of the primarily formed solid is always inevitable, which damages the perfectness of the dendritic structure, and even leads to the formation of the fully refined structure as shown in Fig. 2b. It can be believed that the solute diffusion in the superheated solid is much faster than that in the not superheated solid. Assume that the recalescence occurs in adiabatic condition, and that the solid and the liquid are in equilibrium at the maximum recalescence temperature T_R. The relations below can be derived according to the mass and the energy conservation laws.

$$f_S^R C_S^R + f_L^R C_L^R = C_0 \quad (1)$$

$$f_S^R = (T_R - T_N)/\Delta T_h \quad (2)$$

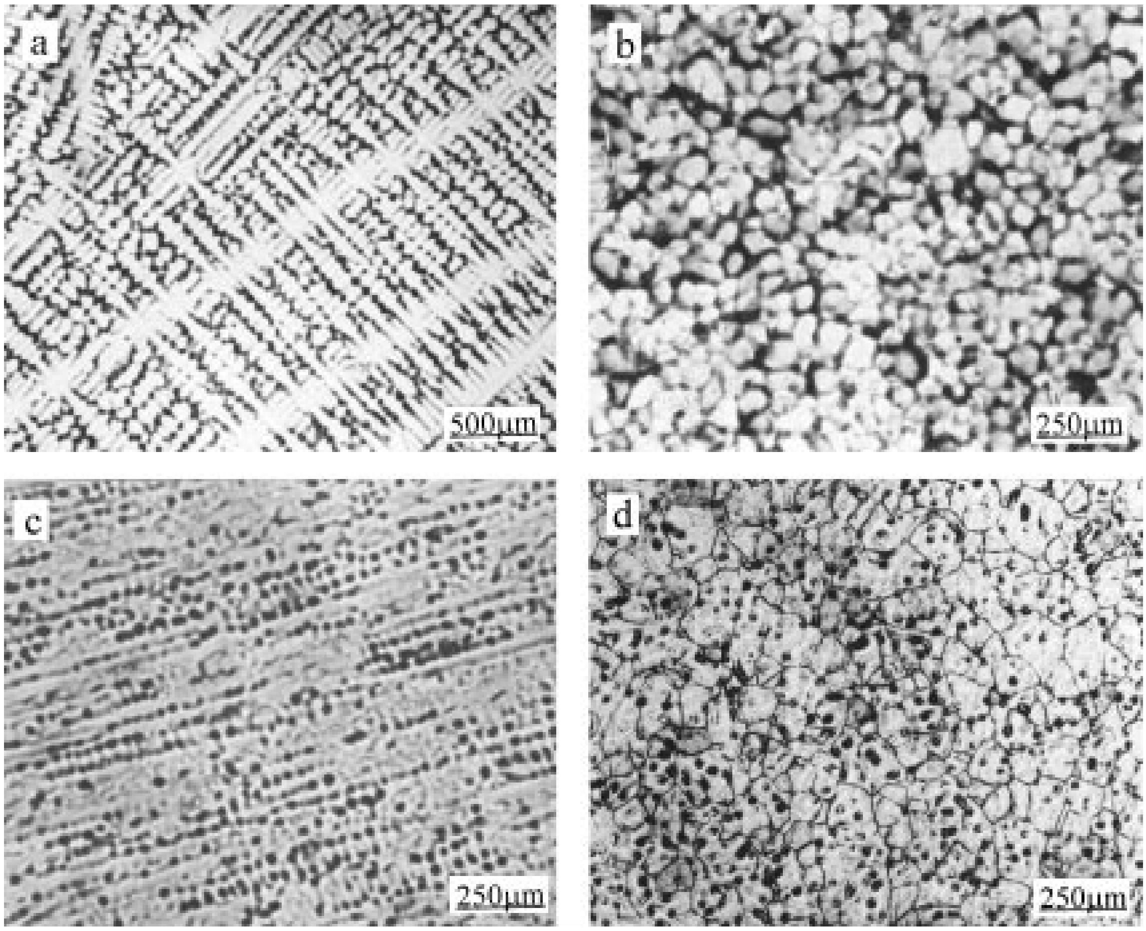

Figure 2 Microstructures of the alloy undercooled by (a) 13 K (b) 48 K (c) 155 K (d) 200 K.

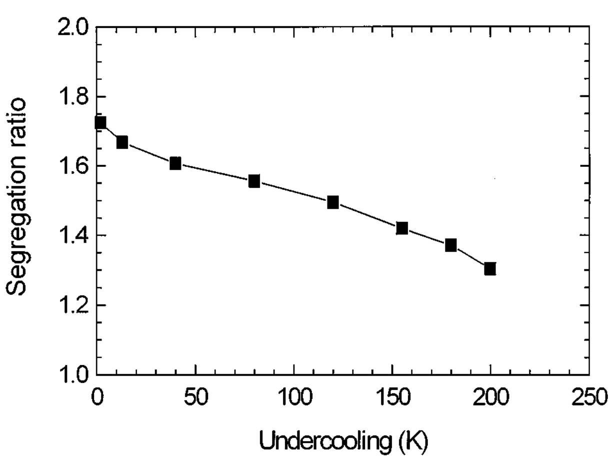

Figure 3 The dendrite segregation ratio of the alloy.

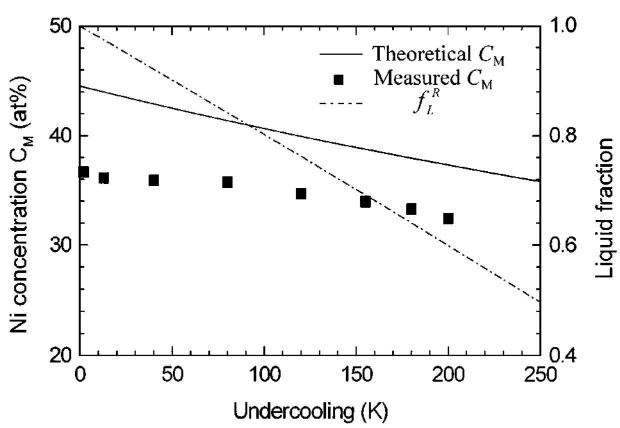

Figure 4 Nickel concentration at the center of dendrite arms, C_{M}, and the liquid mass fraction at the end of recalescence, $f_{\mathrm{L}}^{\mathrm{R}}$.

where $C_{\mathrm{L}}^{\mathrm{R}}$, $C_{\mathrm{S}}^{\mathrm{R}}$ are the solute concentration of the liquid and the solid at T_{R}, respectively, $f_{\mathrm{S}}^{\mathrm{R}}$, $f_{\mathrm{L}}^{\mathrm{R}} = 1 - f_{\mathrm{S}}^{\mathrm{R}}$ the mass fraction of solid and liquid, rspectively, and T_{N} the temperature prior to nucleation. The hypercooling limit $\Delta T_{\mathrm{h}} = \Delta H / C_{\mathrm{P}}$ in which ΔH is the heat of fusion, and C_{P} the specific heat of the alloy.

Using the thermophysical data of $Cu_{70}Ni_{30}$ provided in Ref. 9, we can calculate the nickel concentration of solid at T_{R}, $C_{\mathrm{S}}^{\mathrm{R}}$, and the mass fraction of liquid $f_{\mathrm{L}}^{\mathrm{R}}$ (Fig. 4). If the diffusion in solid in the slow solidification stage can be neglected, $C_{\mathrm{S}}^{\mathrm{R}}$ should also be equal to the solute concentration at the center of dendrite stem at room temperature, C_{M}. The solid squares in Fig. 4 represent the corresponding measurement results. The fact that the actual C_{M} is lower than $C_{\mathrm{S}}^{\mathrm{R}}$ can be attributed to the disability for the actual recalescence temperature to reach the theoretical value, and especially the inevitable solid diffusion during the slow solidification phase.

At a given cooling rate, the liquid fraction at the end of recalescence $f_{\mathrm{L}}^{\mathrm{R}}$ decreases with increasing undercooling, which means a shortened solidification time. In addition the decrease of dendritic substructure size

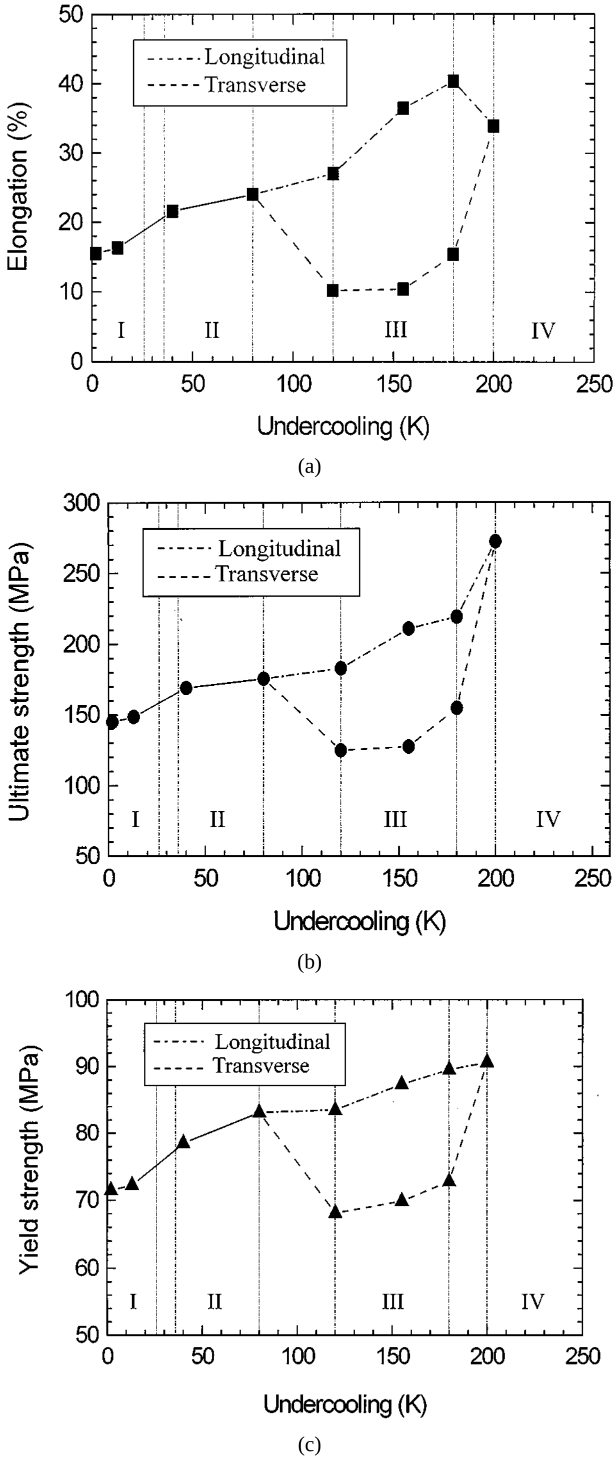

Figure 5 Mechanical properties *vs* undercooling (a) elongation (b) ultimate tensile strength (c) yield strength, where I—coarse equiaxed dendrites, II—refined granular grains, III—columnar dendrites, IV—refined quasi-spherical grains. The structure in the regions not marked consists of the mixture of the structures in the neighboring regions.

with undercooling [12] makes the segregative length shortened. So the deviation of the solute concentration at the boundaries from the average value becomes lightened, i.e. segregation ratio decreases (Fig. 3).

3.3. Mechanical properties

Fig. 5 shows the mechanical properties of $Cu_{70}Ni_{30}$ alloy at different undercooling. The structure at the undercooling lower than 26 K consists of coarse equiaxed dendritic crystals whose size is as large as several millimeters. Under the action of tensile stress, heavy segregation of copper in the structure create a favorable condition for crack to nucleate and rapidly propagate along boundaries, leading to the intergranular fracture. The uneven micro deformation concentrated at the boundary area make it possible that the dendrite morphology can still be observed on the fractograph (Fig. 6a). In this case neither elongation nor strength is high.

In the undercooling range of 36–80 K, grain refinement make the intergranular segregation decrease considerably, and the grain boundary is no longer the favorable way for the spread of crack in each case. Fig. 6b illustrates the fractograph at undercooling 80 K. It is clear that a mixture of transcrystalline and intergranular fracture occurs in the tensile test. So in this undercooling range good mechanical properties appear. Compared with the values at zero undercooling, δ and σ_b increase 54.97% and 21.15% at undercooling 80 K.

Strong directionality shows in the mechanical properties of the ingot solidified in the undercooling range 120–180 K where the structure consists of coarse columnar dendrites. When tensile stress is approximately parallel to the primary dendrite arms, the influence of the constituent inhomogenity of the alloy on mechanical properties is lessened. However, when undercooling is smaller than 150 K, the remelting of solid due to chemical superheating is still heavy, and causes a severe local destruction in the primary dendrite stems, which makes the increasement of mechanical properties limited. The rapid rise of the properties occurs in the undercooling range 120–180 K. The maximum elongation, as high as 40.39%, is obtained at undercooling 180 K, and it is 160.58% greater than the value at zero undercooling. Fig. 6c shows the corresponding fractograph. The fine ductile tearing ridges imply the existence of a large deformation strengthening.

By contrast, when the tensile stress perpendicular to the primary arms is exerted, cracks can readily propagates along the grain boundaries (Fig. 6d). The elongation and strength are even lower than the values at low undercoolings.

The solidification above the critical undercooling 200 K induces the quasi-spherical grains and the abrupt decrease of the grain size. The corresponding rise of grain boundary area and the emergence of twins inside grains strengthen the material. As a result the ultimate strength reaches its maximum 272.47 MPa, which is 87.91% and 24.19% higher than the ultimate strength at 0 K undercooling and 180 K (longitudinal) respectively, whereas compared with the value at 180 K undercooling, the elongation decreases by 15.99%. A typical ductile cellular fractograph is observed (Fig. 6e).

With the increasing of undercooling, the yield strength $\sigma_{0.2}$ varies in the same way with the ultimate strength. However, the considerable variation is not found in $\sigma_{0.2}$. Its maximum present at undercooling 200 K is only 26.74% higher than the value at zero undercooling.

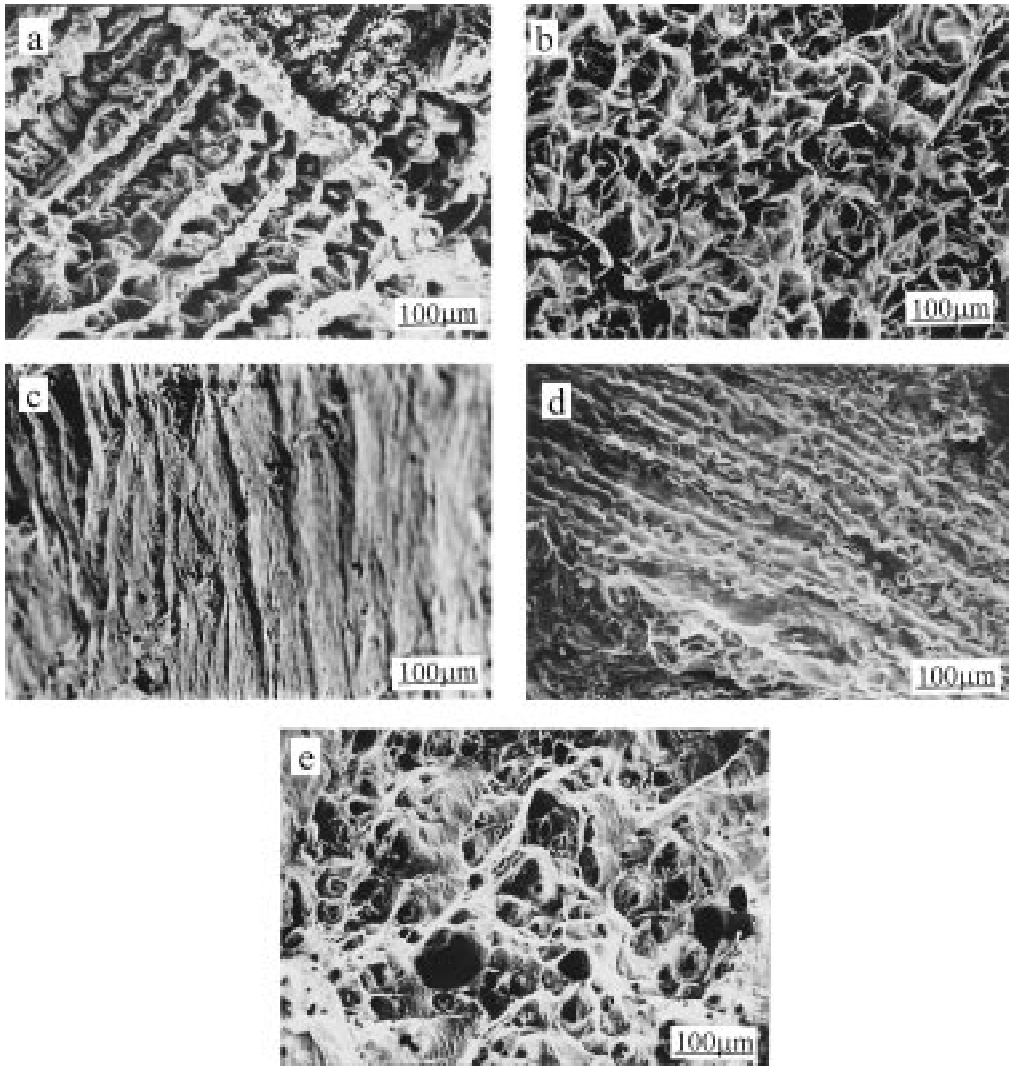

Figure 6 Tensile fractographes of the alloy undercooled (a) 13 K (b) 80 K (c) 180 K (longitudinal) (d) 155 K (transverse) (e) 200 K.

4. Conclusions

(1) The solidification structure of $Cu_{70}Ni_{30}$ alloy is the strong function of undercooling prior to nucleation. When undercooling is in the range of 36–80 K or above 200 K, grain refinement occurs, whereas the melts undercooled in 120–180 K solidify into columnar dendritic crystals.

(2) The theoretically calculated and experimental results indicate that the microsegregation decreases with increasing undercooling constantly, which is favorable for the improvement of the mechanical properties. However, the sophisticated evolution of solidification structure can lead to completely distinct fracture mode when undercooling changes. As a result the as-solidified mechanical properties do not vary monotonically.

(3) The maximum elongation and ultimate strength are obtained at the undercooling 180 K (longitudinal) and 200 K respectively, being 160.58% and 87.91 higher than the corespondent values at zero undercooling. However, the influence of undercooling on the yield strength is not as significant as on the elongation and the ultimate strength.

(4) It is suggested that for the ordinary castings of $Cu_{70}Ni_{30}$, the undercoolings should be chosen in the range of 36–80 K and preferentially above 200 K, while the undercooling range 120–180 K be only appropriate for the castings merely bearing unidirectional stress.

References

1. R. W. CAHN, in "Rapidly Solidified Alloys," edited by H. H. Lieberman (Marcel Dekker, Inc., New York, 1993) p. 1.
2. D. M. HERLACH, *Mater. Sci. Eng.* **R12** (1994) 177.
3. T. Z. KATTAMIS and M. C. FLEMINGS, *AFS Trans.* **75** (1967) 191.
4. Z. Z. XI, G. C. YANG and Y. H. ZHOU, *Chinese J. Mater. Res.* **12**(1) (1998) 37.
5. A. LUDWIG, I. WAGNER, J. LAACKMANN and P. R. SAHM, *Mater. Sci. Eng.* **A178** (1994) 299.
6. Y. WU, T. J. PICCONE, Y. SHIOHARA and M. C. FLEMINGS, *Metall Trans.* **19A** (1988) 1109.
7. R. WILLNECKER, D. M. HERLACH and B. FEUERBACHER, *Phys. Rev. Lett.* **62** (1989) 2707.
8. G. D. MERZ and T. Z. KATTAMIS, *Metall. Trans.* **8A** (1977) 295.
9. J. F. LI, Y. C. LIU, Y. L. LU, G. C. YANG and Y. H. ZHOU, *J. Crystal Growth* **192** (1998) 462.
10. A. F. NORMAN, K. ECKLER, A. ZAMNON, F. GARTNER, S. A. MOIR, E. RAMOUS, D. M. HERLACH and A. L. GREER, *Acta Mater*. **46** (1998) 3355.
11. J. F. LI, Y. H. ZHOU and G. C. YANG, *J Crystal Growth* **206** (1999) 141.
12. J. F. LI, G. C. YANG and Y. H. ZHOU, *Mater. Res. Bull.* **33** (1998) 141.

Received 8 November 1999
and accepted 2 March 2000